Indian J. Phys. 77A (2), 133–138 (2003)

AN INTERNATIONAL JOURNAL IJPA

Transport characteristics and effect of Ag in controlling thermally activated phase-slip in Ca doped $YBa_2Cu_3O_{7-y}$

D Behera[1]*, S K Dash[2] and N C Mishra[1]

[1]Department of Physics, Utkal University, Bhubaneswar-751 004, Orissa, India

[2]Department of Physics, K B D A V College, Nirakarpur-752 019, Orissa, India

E-mail : dbehera@iopb.res.in

Abstract . DC resistivity of $Y_{1-x}Ca_xBa_2Cu_3O_{7-y}$ and $Y_{1-x}Ca_xBa_2Cu_3O_{7-y}$/Ag composite bulk sinter samples has been studied as a function of applied magnetic field and temperature. A percolative current conduction model was utilized to quantify granularity in the bulk in terms of such parameters like the weak link resistivity across grain boundaries, current path lengthening factor arising due to grain misalignment, and due to voids and cracks. Evolution of these parameters with Ag content in the sample indicates improved grain alignment and reduced structural defects (voids and cracks). The resistive broadening by magnetic field has been described by thermally activated flux creep or flux-flow behaviour which is much reduced in Ag composite sample. Hence the grain boundary which has much technical application is improved by Ag addition.

Keywords : Percolative conduction, flux creep, activation energy.

PACS Nos. : 74.72.Bk, 74.60.Ge, 74.62.Dh

1. Introduction

Since the discovery of high temperature cuprate superconductors, it is established that both charge carriers and oxygen content control the superconducting and normal state properties in these systems. In $YBa_2Cu_3O_{7-y}$ (YBCO) system, the carrier density can be enhanced either by increase of oxygen content or by on-site cationic substitutions with dopants of lower valence state. Ca doping has created much interest in the scientific community as this doping turns an oxygen-deficient YBCO system from insulator to superconductor. On the other hand, Ca doping decreases the oxygen content of the oxygen overdoped samples resulting in the reduction of transition temperature T_c [1,2]. The reduction of oxygen content by Ca doping is countered by extra holes introduced by Ca^{2+} ions [3]. Hence, by partial doping of Ca^{2+} for Y^{3+} in $Y_{1-x}Ca_xBa_2Cu_3O_{7-y}$ ($Y_{1-x}Ca_x$-123) sample, charge carriers introduced by Ca doping is expected to be in-part compensated by a reduction of equilibrium oxygen content [1]. To compensate for the depletion of oxygen content by Ca doping, we add silver in the form of composites in $Y_{1-x}Ca_x$-123 samples. Ag is known to stabilize the oxygen content in the cuprate superconductors. The superconducting Ag composites are considered potential candidates for technical applications due to their increase in critical current density [4], lowering of normal state resistivity [4], better chemical stability and increase of mechanical strength [5].

Cuprate superconductors are granular in nature. The granularity problem can be controlled by various ways and one of the ways is to prepare Ag composites of them. The transport properties of grain boundaries are modified much by Ag composites. In application to electronic circuits grain boundary Josephson junctions have been proved to be highly useful [6]. Grain boundaries in high T_c superconductors are of prime importance for application in cryoelectronics circuits, as well as for high T_c cables and tapes [7].

The cuprate superconductors show two-stage resistive transition– (a) the step part and (b) the tail part. The step part of the resistive transition region, where there is onset of

*Corresponding Author

superconducting transition, remains unaffected under different applied field. With increasing the magnetic field the superconducting transition T_{c_0} (R = 0) shifts to lower temperature side. Strong magnetic field is required to observe an appreciable resistive broadening in oriented and single crystals but similar broadening can be observed in polycrystalline bulk sample with low field ~10 G [8]. This broadening was first quantitatively showed by Tinkham [9]. Latter this feature has been explained successfully by several authors [8-11] through Ambegaokar-Halperin (AH) phase-slip theory. An increase in magnetic field results in the penetration of more magnetic flux lines into the material. This field enhances the Lorentz force that causes more flux lines to move. On the other hand, the tail part is suggested to be associated with link between the grains and extremely sensitive to magnetic field. The flux creep and flux flow model may essentially hold good if the magnetic flux enter into material in the vortex state by bending due to grain boundary or by crystallographic anisotropy [12].

In the present work, we report on the role of Ag in controlling the grain boundary resistivity and modifying the electrical and magnetic properties at the grain boundaries. The typical signature of flux flow resistivity modified in the Ag composite sample is observed.

2. Experimental

The bulk superconductors used in the present study are ($Y_{0.9}Ca_{0.1}$-123) and ($Y_{0.9}Ca_{0.1}$-123)/Ag 10 wt% composite samples. For the preparation of ($Y_{0.9}Ca_{0.1}$-123), the chemicals taken were Y_2O_3, $BaCO_3$, $CaCO_3$ and CuO. They were of high purity (99.9%) except $BaCO_3$ which was 99.8% pure. The samples were prepared by standard solid state reaction of the constituents to their stoichiometry. For the preparation of ($Y_{0.9}Ca_{0.1}$-123)/Ag composite bulk sinters, Ag_2O was mixed with ($Y_{0.9}Ca_{0.1}$-123) powder before the final stage of sintering. The ($Y_{0.9}Ca_{0.1}$-123) pellets prepared were thoroughly ground and mixed with Ag_2O with appropriate proportions to obtain ($Y_{0.9}Ca_{0.1}$-123)/Ag composites. The samples were pressed into pellets, annealed at 920°C for 12 hrs and cooled to 400°C where they stayed for 12 hrs with oxygen flowing. Then the samples were cooled to room temperature at a rate of 2°C/min.

The samples were characterized at room temperature by XRD using CuK_α radiation. The XRD pattern was analyzed and different peaks were identified. The resistivity of the samples was measured with four-probe arrangement, the details of which were discussed in our previous publication [13]. The ρ *vs* T data were taken by a computer controlled data acquisition system during heating of the sample to room temperature. The heating rate was confined to 3 K per minute. Magnetic field was applied perpendicular to direction of measuring current in the range 0–1.1 kG.

3. Results and discussion

3.1. Phase formation :

From the XRD spectrum (Figures 1 and 2), it is observed that many impurity phases which appear in case of $Y_{0.9}Ca_{0.1}$-123 samples are suppressed in $Y_{0.9}Ca_{0.1}$-123/Ag composite sample. Further, the Ag peaks in the XRD spectrum are prominent at the expense of the $Y_{0.9}Ca_{0.1}$-123 peaks. The peaks appearing at 2θ values of 44.2 and 65.0 can respectively be indexed as (200) and (220) peaks of metallic silver. Ag therefore appears as a separate phase at the grain boundaries of $Y_{0.9}Ca_{0.1}$-123. The c-axis lattice parameter remained same for both the systems. This suggests that proper ionic matching of Ca and Y has occurred and Ag remained at the grain boundary in the composite samples. The impurity peak for $CaCu_2O_3$ which has been reported [10] in the system at 2θ= 33.94 is absent in our case as Ag cleans the grain boundaries.

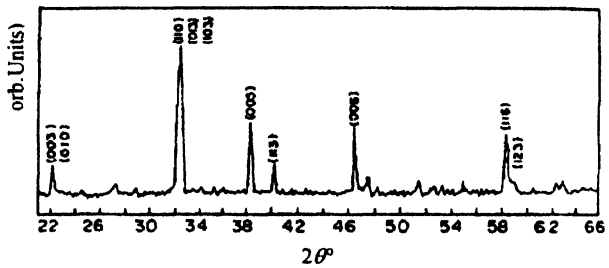

Figure 1. X-ray diffraction pattern of $Y_{0.9}Ca_{0.1}$-123 bulk sinter.

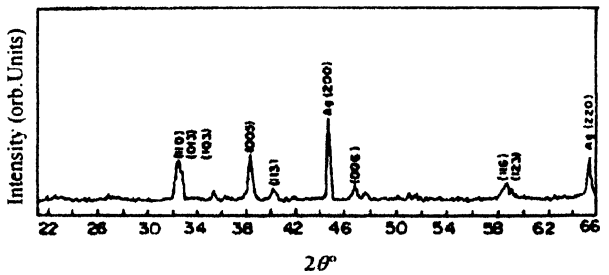

Figure 2. X-ray diffraction pattern of $Y_{0.9}Ca_{0.1}$-123/Ag (10 wt%) composite sample.

3.2. Resistivity studies and charge transfer mechanism :

The temperature dependent electrical resistivity (ρ *vs* T) of $Y_{0.9}Ca_{0.1}$-123 and $Y_{0.9}Ca_{0.1}$-123/Ag (10 wt%) is shown in the Figure 3. Though the onset of superconducting transition occurs at same temperature ($T_{c_{onset}}$ = 84 K) in both the systems, Ag composite one shows the improvement of T_{c_0} (R = 0) from 78 K to 81 K. Addition of Ag in the system does not degrade the transition temperature rather improves the coupling strength and enhances the microstructural modifications [4].

The decrease of T_c in Ca doped YBCO is reported by several authors due to (a) oxygen vacancies [14-16], (b) magnetic scattering centers inducing pair-breaking [1,17-19] and (c) overdoping effect [1,20,21]. In the light of above we

discuss the charge transfer mechanism in Ca doped system that explains the decrease of T_c. From structural refinement data of Wu *et al* [2] it is observed that there is larger shift of O(2) site to Cu(1)-O chains. This O(2) site plays an important role for charge transfer from chain to plane [22]. As a result, hole concentration in Cu(2)-O sheets decreases. Though Ca doping increases total hole concentration but mobile holes at Cu(2)-O sites matters in deciding the transition temperature of the system. Hence in fully oxygenated system, Ca doping decreases the transition temperature.

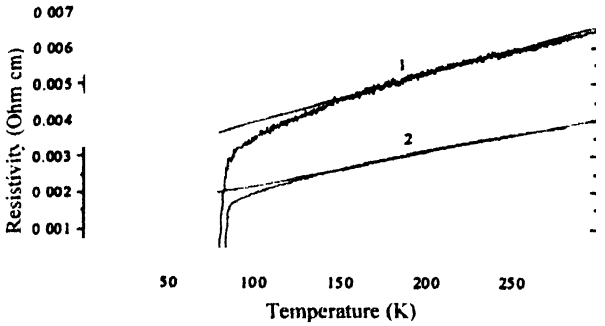

Figure. 3. Temperature dependent of resistivity in (1) $Y_{0.9}Ca_{0.1}$-123 and (2) $Y_{0.9}Ca_{0.1}$-123/Ag (10 wt%) composite sample. Linear fitting of the resistivity in the temperature range 150 to 250 K and extrapolated 0 K gives slope ($d\rho/dT$) and residual resistivity (ρ_0)

The decrease of oxygen content in turn decreases the valence of both Cu(1) and Cu(2) [3]. As oxygen vacancies are created mainly at O(1) site (CuO chain) Cu(1)'s are more affected than Cu(2). The Cu(1)'s with nearby oxygen vacancies become 3-fold oxygen coordinated creating metastable state. For each oxygen vacancy, there will be two nearby Cu(1) ions which are driven to unstable three-fold oxygen coordination. The resulting unstable charge state of these Cu(1) ions can fluctuate between two stable charge states 2+ and 1+. The resulting charge fluctuation in the CuO basal plane induces antiferromagnetically coupled spin fluctuation in the CuO_2 planes. This process basically explains the mechanism of superconductivity that has been discussed in our previous paper [23].

3.3. Estimation of granularity parameters :

From resistivity plots (Figure 3) the normal state resistivity in Ag composites decreases as compared to Ag free sample. In both the cases the normal state resistivity increases linearly with temperature beyond the superconducting order parameter fluctuation (SCOPF) region. The slope of the curves gives $d\rho/dT$ and the linear extrapolation of the curves to $T = 0$ K gives the residual resistivity ρ_0. Based on a percolation current conduction model [24] one can obtain the resistivity

$$\rho = 1/\alpha[\rho_{ab} + \rho_{wl}] \tag{1}$$

where ρ_{ab} is the intragrain resistivity in the ab-plane which has the same value as measured in single crystals. ρ_{wl} is the average weak link resistivity across the grain boundaries. The factor $\alpha = f.\alpha_{str}$ contains contribution of both the path lengthening factors f arising due to blocking of the current across the misaligned surface of the highly anisotropic grains and α_{str} is due to voids and microcracks.

The magnitude of ρ_0, that is a measure of grain boundary resistivity [25], decreases at a faster rate as compared to ρ_{295K} in the Ag composite sample. Within percolation threshold (~20 vol%) for Ag composites, our observation of $\rho_0(0)/\rho_0(Ag) = 1.6$ is lower than $\rho_{295}(0)/\rho_{295}(Ag) = 2.1$, suggests that Ag reduces the grain boundary resistivity faster than the normal state resistivity of the sample. As seen from the Figure 3, the normal state resistivity of the samples is linear with temperature. Following the procedure of Diaz *et al* [24] this linearity of ρ allows us to calculate the parameters ρ_{wl} and α for different samples as shown below. ρ_{wl} is assumed to be independent of temperature above T_c and taking the derivative it gives

$$d\rho/dT = (1/\alpha)(d\rho_{ab}/dT). \tag{2}$$

Assuming the intragranular resistivity ρ_{ab} to have a negligible intercept at 0 K, ρ_{wl} is determined as

$$\rho_0 = (1/\alpha)\rho_{wl}. \tag{3}$$

The parameters ρ_{wl} and α which quantify granularity are evaluated taking $d\rho_{ab}/dT = 0.5$ μ ohm K^{-1} from single crystal measurement [26]. The change in the measured resistivity slope $d\rho/dT$ of the sample gives value of ρ_{wl} and α. It should be noted that the magnitude of ρ_{wl} represents the average weak link resistivity in a granular medium and is the physically relevant resistivity in polycrystalline materials for comparison with models and theories of junctions, weak link structure *etc*. Ag in the composites reduces the weak link resistivity and improve current conduction path in the granular systems as is evident from the Table 1 showing variation of ρ_{wl} and α. The decrease of ρ_{wl} and increase of α with Ag addition indicates that the intergranular contribution to the total resistivity decreases.

Table 1. Variation of the normal state and superconducting parameters in the Ca doped and Ag composite bulk sintered samples.

Ag wt%	ρ_{295K} (mohm cm)	ρ_0 (mohm cm)	$d\rho/dT$ (μ ohm cm K^{-1})
0	6.4	2.60	13.26
10	3.9	1.24	9.34

3.4. Magnetoresistivity and thermally activated flux creep model :

The polycrystalline bulk $Y_{0.9}Ca_{0.1}$-123 sample typically shows a two-stage resistive transition when magnetic field is applied perpendicular to the current direction. As seen from the

Figures 4 and 5, the step part is unaffected by the applied magnetic field and the tail part showing T_{c_0} moves considerably to lower temperature side with large broadening for Ag free sample than Ag composite sample. The sensitiveness decreases in increasing magnetic field [10] which is evident in the Figures 4 and 5.

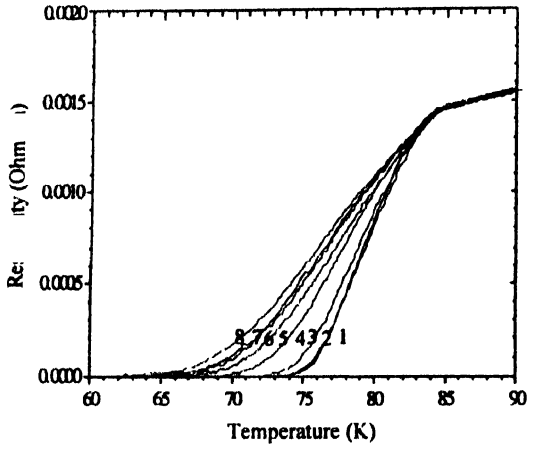

Figure 4. Resistive transition of $Y_{0.9}Ca_{0.1}$-123 sample with varying magnetic fields (1) 0 G (2) 30 G (3) 60 G (4) 140 G (5) 280 G (6) 420 G (7) 565 G (8) 1.1 kG applied in a perpendicular direction to the measuring current.

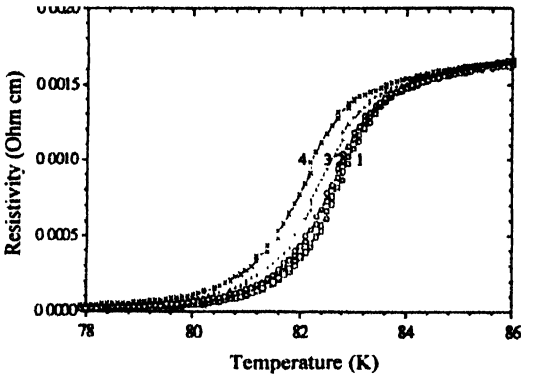

Figure 5. Resistive transition of $Y_{0.9}Ca_{0.1}$-123/Ag (10 wt%) composite sample with varying magnetic fields (1) 0 G (2) 565 G (3) 830 G (4) 1.1 kG applied in a perpendicular direction to the measuring current.

The broadening of the resistive transition observed in $Y_{0.9}Ca_{0.1}$-123 bulk sintered sample in the presence of an external magnetic field is attributed to phase-slip phenomenon due to thermally activated motion of vortices according to AH model [10]. The resistive transition temperature in Ag free Ca doped sample shows the shifting of transition temperature to lower temperature side having large transition width ΔT_c. T_{c_0} shows a marked change from 74 K to 64 K for H = 565 G and to 63 K for H = 1.1 kG. In comparison to Ag free sample (Figure 4), the Ag composite sample (Figure 5) shows a much reduced effect of field at the T_{c_0} region. Though T_{c_0} reduced from 81 K to 79 K for H = 565 G and to 78 K for H = 1.1 kG the tailing and broadening is not pronounced.

In the framework of thermally activated flux creep model, the broadening of the resistive transition can be expressed as [27]

$$\rho(T, H) = \rho_0 \exp[-U_0(T, H)/T], \quad (4)$$

the activation energy $U_0(T, H)$ is both temperature and field dependent. The activation energy due to field dependence is calculated for the samples. The slope of the straight line in the curve ln ρ *vs* $1/T$ (Figures 6 and 7) gives the activation energy $U_0(H)$ for the flux line in different magnetic fields. This energy is observed to decrease for increasing the magnetic field from 0 to 1.1 kG.

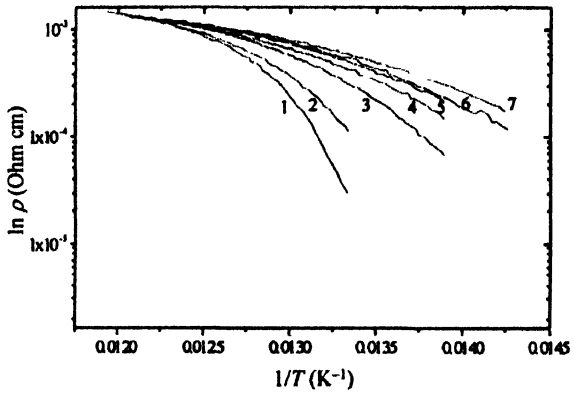

Figure 6. The plot of log ρ *vs* $1/T$ of $Y_{0.9}Ca_{0.1}$-123 with varying magnetic fields 0 G (2) 60 G (3) 140 G (4) 280 G (5) 420 G (6) 565 G (7) 1.1 kG applied in a perpendicular direction to the measuring current. The slope at the linear region gives activation energy U_0.

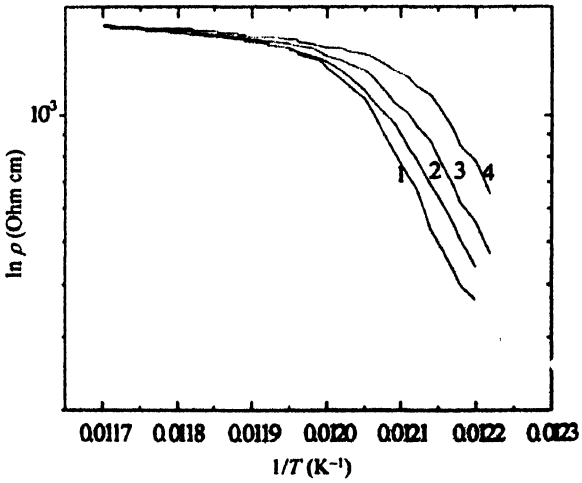

Figure. 7. The plot of log ρ *vs* $1/T$ of $Y_{0.9}Ca_{0.1}$-123/Ag (10 wt%) composite sample with varying magnetic fields (1) 0 G (2) 565 G (3) 830 G (4) kG applied in a perpendicular direction to the measuring current. The slope at linear region gives activation energy U_0.

In Figures 8 and 9, the magnetic field dependent activation energy has been plotted as a function of applied magnetic field for Ag free $Y_{0.9}Ca_{0.1}$-123 and Ag composite $Y_{0.9}Ca_{0.1}$-123 sample. The dependence of U_0 is predicted to obey a power law of the form $U_0(H) \sim H^{-\alpha}$ from where the exponent

is calculated to be 0.18 and 0.09 (Figures 8 and 9) for $Y_{0.9}Ca_{0.1}$-123 and $Y_{0.9}Ca_{0.1}$-123/Ag composites bulk sinters respectively. The value of α is in agreement with those found for YBCO [12,28] with magnetic field applied perpendicular to the current direction. Ag composite sample shows higher activation energy than Ag free sample, it therefore requires higher magnetic field to produce same broadening of the resistive transition as Ag free sample.

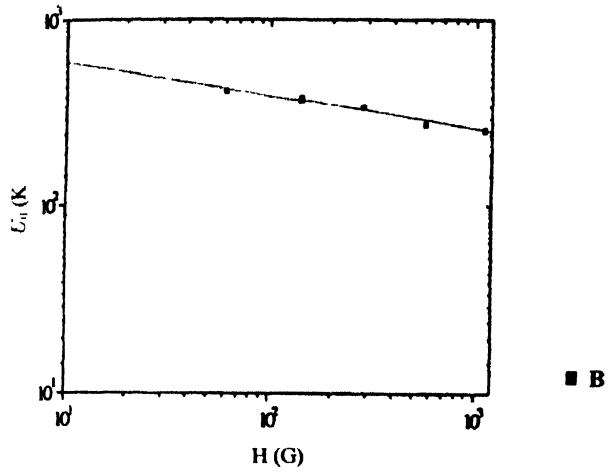

Figure. 8. The magnetic field dependence of activation energy $U_0(H)$ in $Y_{0.9}Ca_{0.1}$-123 at temperature close to T_{c_0}. The power law dependence of $U_0(H) \sim H^{-\alpha}$ gives $\alpha = 0.18$.

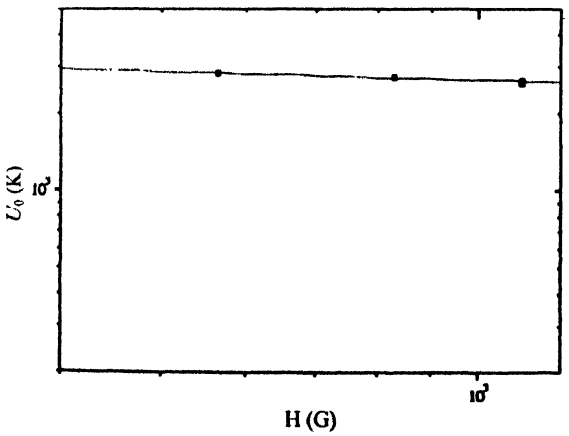

Figure. 9. The magnetic field dependence of activation energy $U_0(H)$ in $Y_{0.9}Ca_{0.1}$-123/Ag (10 wt%) composite at temperature close to T_{c_0}. The power law dependence of $U_0(H) \sim H^{-\alpha}$ gives $\alpha = 0.09$.

The lower part of the foot structure shows the sample inhomogeneity – the sample containing both the grain and grain boundary junctions with distinctly different properties. The local current and magnetic field *i.e.* the ratio of local current density and the magnetic field dependent Josephson critical current control the binary status of the junction. The formation of stress field in Ca doped samples causes a local flux pinning at the unit cell level [29] that is further enhanced by Ag composites.

4. Conclusion

The resistive broadening by magnetic field has been described by thermally activated flux creep or flux-flow behaviour. The pinning energy due to thermally activated process has been determined. The observed increase of activation energy and reduced broadening of resistive transition can be interpreted as the arrest/slow down of the vortex motion i.e. flux line lattice is more rigid in Ag composite sample than flux line lattice in Ag free sample below their critical temperature.

Acknowledgments

The authors gratefully acknowledge the financial support from the University Grants Commission, New Delhi, India.

References

[1] J T Kucera and J C Bravman *Phys. Rev.* **B51** 8582 (1995); V P S Awana and A V Narlikar *Phys. Rev.* **B49** 6353 (1994)

[2] X S Wu, S S Jiang, J Lin, J S Liu, W M Cheu and X Jin *Physica* **C309** 25 (1998)

[3] D H Ha, S Byon and Y Kim *Physica* **C333** 72 (2000)

[4] D Behera, K Patnaik and N C Mishra *J. Supercond.* **11** 641 (1998)

[5] R Pinto, P R Apte, M S R Rao, Ramesh Chandra, C P D'Souza, S P Pai, L C Gupta and R Vijayaraghavan, K I Gnanasekhar and M Sharon *Appl. Phys Lett.* **68** 1006 (1996)

[6] *Proc. Europian Conf. on Appl. Supercond.* **Vol 158** (eds.) H Rogalla and D H A Blank 1997

[7] H Hilgerkanp and J Manhart *Appl. Phys. Lett.* **73** 265 (2000)

[8] C Gaffeny, H Petersen and R Bednar *Phys. Rev.* **B48** 3388 (1993)

[9] M Tinkham *Phys. Rev. Lett.* **61** 1658 (1988)

[10] H Shakeripour and M Akhavan *Supercond Sci. Technol.* **14** (2001) 234

[11] H S Gamchi,G J Rusell and K N R Taylor *Phys. Rev.* **B50** 12950 (1994)

[12] Y Koike, M Masuzawa, H Sunagawa, T Noji, H Kawabe and N Kobayashi *Jpn. J. Appl. Phys.* **29** L408 (1990)

[13] D Behera, K Patnaik and N C Mishra *Modern Phys. Lett.* **B15** 69 (2001)

[14] B Fisher, J Genossar, C G Kuper, L Patlagan, G M Reisner and A Knizhnik *Phys. Rev.* **B47** 6054 (1993)

[15] Y Sun, G Strasser and E Gornik *Physica* **C223** 14 (1994)

[16] H Yakabe, M Kosuge, J Tsujino, Y Shiohara and N Koshizuka *Jpn. J. Appl. Phys.* **34** 4754 (1995)

[17] T Zenner, H Peizer, B Obst, J Bittner, P Schweiss, T Wolf, M Klaser, G Miller-Vogt, H Claus and H Wiihl *J. Low Temp. Phys.* **105** 909 (1996)

[18] A Sedky, Anurag Gupta, V P S Awana and A V Narlikar *Phys. Rev.* **B58** 12495 (1998)

[19] A K Sarin Kumar, T Itoh, M Kawasaki and H Koinuma *Physica* **C349** 83 (2001)

[20] J L Tallon, C Bernhard, H Shaked, R L Hitterman and J D Jorgensen *Phys. Rev.* **B51** 12911(1995)

[21] K Widder, D Berner, J Munzel, H P Geserich, M Klaser, G Muller-Vogt and Th Wolf *Physica* **C267** 254 (1996)

[22] Y Takura, J B Torrance, T C Huang and A I Nazzal *Phys. Rev.* **B38** 7156 (1988)

[23] H P Mohapatra, D Behera, B Dash, N C Mishra and K Patnaik *Physica* **C185** 739 (1991)

[24] A Diaz, J Maza and F Vidal *Phys. Rev.* **B55** 1209 (1997)

[25] A Diaz, A Pomer, G Domarco, J Maza and J F Vidal *Appl Phys Lett.* **63** 1684 (1993)

[26] A Kapitulnik *Physica* **C153** 520 (1988)

[27] H E Horng, H H Sung, B C Yao and H C Yang *Physica* **C185** 2221 (1991)

[28] H H Sung, H C Yang, T R Yang, B C Yao and H E Horng *Physica* **C185** 2223 (1990)

[29] A Radhika Devi, V Seshu Bai, P V Patanjali, R Pinto, N Hari Kumar and S K Malik *Supercond. Sci.Technol.***13** 935 (2000)